
**Separation Science and Technology**
Publication details, including instructions for authors and subscription information:
http://www.informaworld.com/smpp/title~content=t713708471

# Nitrogen-15 Fractionation by Countercurrent Exchange between Liquid $N_2O_3$-$N_2O_4$ Mixtures and Their Vapor Phases under Pressured Conditions

Michael Prencipe[a]; William Spindel[b]; Takanobu Ishida[c]
[a] DEPARTMENT OF CHEMISTRY, BROOKLYN COLLEGE CITY UNIVERSITY OF NEW YORK, BROOKLYN, NEW YORK [b] NATIONAL ACADEMY OF SCIENCES, WASHINGTON, D.C. [c] DEPARTMENT OF CHEMISTRY, STATE UNIVERSITY OF NEW YORK, NEW YORK

**To cite this Article** Prencipe, Michael , Spindel, William and Ishida, Takanobu(1985) 'Nitrogen-15 Fractionation by Countercurrent Exchange between Liquid $N_2O_3$-$N_2O_4$ Mixtures and Their Vapor Phases under Pressured Conditions', Separation Science and Technology, 20: 7, 489 — 511
**To link to this Article: DOI:** 10.1080/01496398508068233
**URL:** http://dx.doi.org/10.1080/01496398508068233

SEPARATION SCIENCE AND TECHNOLOGY, **20**(7 & 8), pp. 489-511, 1985

# Nitrogen-15 Fractionation by Countercurrent Exchange between Liquid $N_2O_3$–$N_2O_4$ Mixtures and Their Vapor Phases under Pressured Conditions

MICHAEL PRENCIPE

DEPARTMENT OF CHEMISTRY
BROOKLYN COLLEGE
CITY UNIVERSITY OF NEW YORK
BROOKLYN, NEW YORK 11210

WILLIAM SPINDEL

NATIONAL ACADEMY OF SCIENCES
WASHINGTON, D.C. 20418

TAKANOBU ISHIDA

DEPARTMENT OF CHEMISTRY
STATE UNIVERSITY OF NEW YORK
STONY BROOK, NEW YORK 11794



**Abstract**

The nitrogen isotope exchange system for $^{15}N$-fractionation consisting of liquid mixtures of $N_2O_3$ and $N_2O_4$ and the vapor phase in equilibrium with the liquid ($NO/N_2O_3$ system) has been studied at temperatures between −9 and 20°C under various pressures below 4 atm. A countercurrent isotope exchange apparatus and an associated product refluxer system are described. At 15°C the effective separation factor, $\alpha_{eff}$, increases from 1.006 at 1 atm to 1.030 at 2.7 atm and levels off thereafter. The observed $\alpha_{eff}$ values are in good agreement with recent spectroscopic data. The height equivalent of theoretical plate (HETP) correlates well with the linear flow rate of gas phase, showing a dominant diffusion-control of the overall exchange rate. At 15°C the HETP of the $NO/N_2O_3$ system under 3~4 atm can be smaller by factors of 7 to 10 than that of the Nitrox ($NO/HNO_3$ exchange) system having the same product rate, rendering the former system a possibility for significantly smaller plant volume.



 0149-6395/85/2007-0489$3.50/0

## INTRODUCTION

Nitrogen of natural abundance consists of 99.635% $^{14}N$ and 0.365% $^{15}N$. Besides its use as a tracer in chemical, biomedical, agricultural, and environmental research, highly enriched $^{15}N$ has been proposed for use in nuclear fuel elements and breeder reactor material at various stages of the development of nuclear energy (*1–4*), primarily due to two favorable nuclear properties of $^{15}N$: The thermal neutron capture cross-section of $^{15}N$ is three orders of magnitude smaller than that of $^{14}N$, and the (n,p) reaction of fast neutrons with $^{14}N$ results in significant production of long-lived, β-active $^{14}C$ while this problem is nonexistent with $^{15}N$. Although the nuclear power enterprise in the United States is presently moribund, there will of necessity be renewed interest in utilizing nuclear energy sources and a likely need for an efficient, practical, large-scale process for fractionating $^{15}N$ as fossil energy reserves diminish.

The possibility of enriching $^{15}N$ by isotope exchange between NO and $NO_2$ was first suggested by Urey and Greiff (*5*) and first demonstrated in a gaseous thermal diffusion column by Taylor and Spindel (*6*). The two-phase exchange system represented by Reaction I

$$^{15}NO(g) + {}^{14}N_2O_3(l) \rightleftarrows {}^{14}NO(g) + {}^{15}N{}^{14}NO_3(l) \qquad (I)$$

was studied by Monse, Spindel, Taylor, and their co-workers (*7–10*).

The system actually involves other nitrogen oxides as well: Near the ambient temperature the liquid phase conists of $N_2O_3$ and $N_2O_4$, while the gas phase is composed of NO, $NO_2$, $N_2O_3$, and $N_2O_4$ (*11, 12*). The effective single-stage separation factor, $\alpha_{eff}$, thus depends on both temperature and pressure. Monse and his co-workers (*8*) measured $\alpha_{eff}$ under the atmospheric pressure by means of the countercurrent flow method of two phases in packed and bubble-cup columns, which yielded $\alpha_{eff}$ ranging from 1.030 at −8.5°C to 1.016 at +14°C. Their single-stage equilibration measurements (*10*) of $\alpha_{eff}$ demonstrated a significant pressure dependence of $\alpha_{eff}$, e.g., at 23°C, $\alpha_{eff}$ = 1.017 and 1.030 at 2.1 and 7.4 atm, respectively.

Compared to the widely used $^{15}N$ separation method of the Nitrox process, i.e., the exchange between gaseous NO and aqueous $HNO_3$ (*13–15*), Reaction I offers the faster overall exchange rates. At a comparable flow rate of 30 mmol nitrogen/min · $cm^2$ and under atmospheric pressure, the height equivalent of the theoretical plate (HETP) for the $NO/N_2O_3$ system at −9°C is one-third of that for the $NO/HNO_3$ system at 25°C (*8*). In addition, a theoretical study of $\alpha_{eff}$ by Ishida and Spindel (*16*) confirmed Monse's earlier findings (*10, 17*) that $\alpha_{eff}$ could be generally

enhanced by increasing the partial pressure of NO. According to the study, the effect should be especially significant near the ambient temperatures until $\alpha_{eff}$ finally levels off at sufficiently elevated pressures. The $NO/N_2O_3$ system under elevated pressures may thus offer column volumes and throughputs such that they may make the process competitive with the Nitrox process.

In this paper we report on the special design considerations necessitated by the use of elevated pressures and on the effects of pressure and temperature on the HETP and $\alpha_{eff}$, and their implications.

## APPARATUS

The apparatus used for this study, schematically shown in Fig. 1, consists of a packed exchange column and its associated systems coupled with an enriched product refluxer system. They were constructed in principle after the Pyrex design used by Monse, Spindel, Kauder, and Taylor (*8*) (hereafter referred to as M.S.K.T.) for their study of the exchange reaction under atmospheric pressure. The exchange column (EXC in Fig. 1) was set up for countercurrent flows of the liquid and gas phases. The liquid was obtained by equilibrating $NO_2$ liquid of natural isotopic abundance from a supply tank against the gas phase leaving the exchange column. Nitrogen-15 enriches in the liquid. From the product (bottom) end of the column the liquid was led into a refluxer column (PRC), in which it was reduced by $SO_2$ to the gas phase of the appropriate chemical composition, which is dominated by NO in most cases, and the gaseous output of the refluxer was returned to the bottom of the exchange column. The gas effluent of the exchange column was not refluxed. The natural abundance level was thus maintained at the top of the exchange column, while the enrichment level at the product end increased toward a steady value. This was followed as a function of time.

Several innovations had to be built into our system to accommodate the elevated pressures. The design pressure used was 15 atm. The entire system was constructed from stainless steels of Type 316, Type 304, and Carpenter-20; Teflon; and O-rings fabricated from Viton of grade V494. Thick disks of annealed Pyrex were used for small viewport windows. All intercolumn connections were made by means of flanges and Cajon VCO fittings, and the stainless steel parts were otherwise Heliarc-welded together.

The innovations needed fell into two categories. The first was a result of the loss of visual observations of activities occurring inside the columns. They involved use of a thermistor for the reaction (reduction) zone

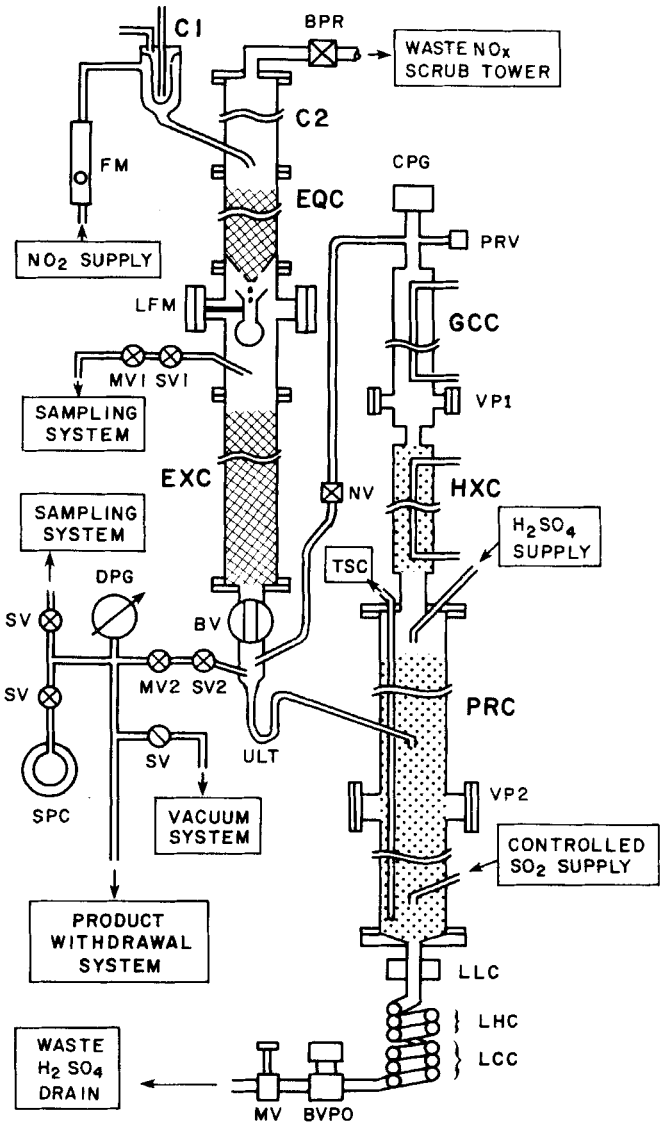


FIG. 1. Schematic diagram of exchange and product-refluxer systems for operation under elevated pressures. Each column is thermostatted by means of fluid jackets, fluid coils, and electric heaters, but they are not shown for the sake of clarity. BPR = backpressure regulator (316 SS), Fairchild-Hiller Industries; BV = ball valve (Teflon, 316 SS); BVPO = ball valve, pneumatically operated; CPG = capacitance pressure gauge (Setra Model 204E, 0–1,000 psia); C1 = condenser, for $NO_2$ (316 SS); C2 = condenser, waste end (316 SS); DPG = diaphragm pressure gauge, 0–760 torr (316 SS); EQC = equilibrator column for

control in the refluxer, use of a magnetically actuated liquid-gas interface level control (LLC) at the bottom of the refluxer, and a new design of the liquid flow-rate measuring cup (LFM).

***Reaction Zone Control by Thermistor.*** In M.S.K.T.'s apparatus (*8*) the reaction zone control was done by optical detection of $NO_2$ in the zone. In the present apparatus the level of the reaction zone in the product refluxer was maintained to within $\pm 1$ cm of a set level by using a thermistor as a probe for detecting the heat generated by the exothermic reflux reactions and by automatically opening and closing a pneumatically actuated bellows-sealed shut-off valve located on an $SO_2$ side line running parallel to a main $SO_2$ feed line, the latter being set at a fixed flow rate. A 10-k $\Omega$ thermistor, immersed in a silicone oil contained in a well made of a ¼"-o.d. Carpenter-20 tubing, was used as an input resistance of a Schmidt trigger circuit. A viewport (VP2) was installed for visual observation of the effectiveness of this reaction zone control method. The method has proved so efficient and reliable that the viewport may be eliminated from future designs of refluxer column.

***Liquid-Gas Interface Level Control.*** Hot sulfuric acid of medium concentrations (8~10 *M*) accumulates at the bottom of the product refluxer (PRC). A proper level of the acid has to be maintained to prevent



---

liquid (316 SS, 20 cm long × 1.55 cm i.d., packed with Podbielniak SS Helipak No. 3013); EXC = exchange column (316 SS, 50 cm long × 1.55 cm i.d., packed with Podbielniak SS Helipak No. 3013); FM = flowmeter, for $NO_2$ (Guarded Pyrex, 316 SS ball); GCC = gas conditioning column (316 SS); HXC = heat exchanger column (316 SS, 3/16 Pyrex helices); LFM = liquid flowmeter; LCC = liquid cooling coil ($H_2SO_4$-carrying Carpenter 20 SS tubing, ⅜" o.d., and coolant-carrying copper tubing, ⅜" o.d., coiled and silver-soldered together); LLC = liquid level controller; LHC = liquid heating coil (constructed in the same manner as LCC); MV = metering valve (316 SS); MV1 = metering valve, for sampling at depleted end (316 SS); MV2 = metering valve, for sampling and product withdrawing at product end (316 SS); NV = needle valve (316 SS); PRC = product refluxer column (Carpenter 20 SS, 1½" pipe, Schedule 40, 38½" long, with Teflon-gasketed Carpenter 20 SS flanges, packed with ¼" Pyrex helices); PRV = pressure relief valve (316 SS); SPC = spectrophotometric cell, thermostatted (Pyrex, Teflon, Viton-494, 316 SS); SV = shut-off valve (316 SS); SV1 = shut-off valve, for sampling at natural abundance end (316 SS); SV2 = shut-off valve, for sampling and product withdrawing at product end (316 SS); TSC = five thermistors (Encased in ¼" o.d. Carpenter-20 tubings with sealed bottom ends, positioned at five levels along the length of PRC column. One is used for control of the reaction zone and the others used in the cooling/heating fluid-flow control circuits.); ULT = U-tube liquid trap; VP1 = view port (¾" o.d. × ¼" annealed Pyrex windows, Teflon gaskets); VP2 = view port (1¼" o.d. × ⅜" annealed Pyrex windows, Teflon gaskets, and Carpenter 20 SS flanges).

$SO_2$ from escaping into the acid waste line. This was accomplished by means of a specially designed liquid level sensor (LLC), which detects the high and low levels of the liquid-gas interface and consequently opens and closes a pneumatically operated ball valve (VBPO).

***Liquid Flow Rate Measuring Cup.*** The flow rates of liquid phase were determined from the liquid density (cf. Results and Discussion) and the time it takes to fill a calibrated volume (1.61 ± 0.01 mL) of a Pyrex measuring cup positioned to receive all drops coming out from the bottom of the equilibrator column (EQC). A calibration mark was etched across the narrowed neck of the cup. A set of two small viewports facing each other were placed at the level of the calibration mark. The viewpoints were fabricated from modified Cajon ¾" VCO fittings, annealed ¼" thick Pyrex disks, and Teflon washers. When the cup was not in use it was kept upside down by rotating it by means of a packless magnetic coupler.



The modifications of the second category were necessitated by the needs for keeping $SO_2$ from condensing under elevated pressures.

In order to maintain the required $SO_2$ feed rate against an elevated pressure, correspondingly high pressures of $SO_2$ had to be maintained in the $SO_2$ supply tank. Also, the partial pressure of $SO_2$ in the lower end of the refluxer column, where presumably the only gas present is $SO_2$, must be maintained at the value of the total pressure. The vapor pressure of $SO_2$ is 15 atm at 73°C. The reflux reaction is exothermic. These considerations led to (a) use of Carpenter-20 stainless steel as a construction material for the refluxer column, (b) use of a multizoned temperature control system for the refluxer column, (c) introduction of a heat exchange column (HXC) to the refluxing system, and (d) insertion of heating (LHC) and cooling (LCC) coils on the waste $H_2SO_4$ line.

Carpenter-20 is a niobium- and tantalum-containing stainless steel which withstands 4~12 *M* $H_2SO_4$ at temperatures up to about 110°C. Nitric acid and oxides of nitrogen have no effect on Carpenter-20. However, the heat generated in the reaction zone would raise the temperature by ~30°C, i.e., to about 100°C, unless appropriate cooling is provided. The chemical composition of the gas returning to the exchange column is controlled by adjusting the temperature of the gas-conditioning column (GCC) and the flow rate of the scrubbing (5 *M*) sulfuric acid. The flow rate of $H_2SO_4$ actually used ranged from 2 to 3 mL/min, depending on the operating conditions of the exchange column.

Since the sulfuric acid which accumulates in the bottom of the refluxer column is in direct contact with $SO_2$, the temperature of the acid has to be maintained above the required minimum level. Yet, the acid has to be at the ambient temperature before it reaches the ball valve (BVPO) which, because it is made of Type 316 stainless steel, easily reacts with hot sulfuric acid. To satisfy both requirements, ⅜″ o.d. Carpenter-20 tubing was wound into two coils. The upper coil (LHC) was wound and brazed together with a length of ⅜″ o.d. copper tubing, the latter providing the required heating. The lower coil (LCC) was constructed similarly, but the copper tubing carried cooling water.

## PROCEDURES

### Experimental

Before starting a run, the packing of the exchange column was wetted by closing the ball valve (BV) and flooding the column with liquid $N_2O_4$. The composition of the liquid phase and the corresponding total pressure were gradually brought to desired levels by operating the reflux system.

During a run, $NO_2$ is supplied from a tank (sometimes heated) at a controlled flow rate and then chemically equilibrated against the gas leaving the exchange column in the equilibrator column. The gas stream left the system through a backpressure regulator (BPR), which is our means for controlling the system's total pressure. The pressure was monitored at two points, one at the inlet of BPR by means of a diaphragm test gauge and the other at the top of the refluxer system by means of a capacitance gauge (CPG) located on the return path of refluxed gas. At the flow rates we employed, the total pressure drop across the exchange and equilibrator columns were within the precision of the diaphragm gauge, i.e., 0.1 atm. The total pressures ($p_t$) were read to $\pm 0.02$ atm on the capacitance gauge. Temperature of the exchange column system was monitored and recorded on a set of calibrated copper-constantan thermocouples.

The overall enrichment by the exchange column was determined as a function of time by periodically sampling the gases from the top (through SV1 and MV1) and the bottom (through SV2 and MV2) of the column, reducing each sample to $N_2$, by slowly passing it through a quartz chamber filled with copper turnings and copper(II) oxide and kept at

800°C, and analyzing the $N_2$ gases for $^{15}N/^{14}N$ ratio using a Consolidated-Nier Model 21-201 isotope ratio mass spectrometer. The sampling was continued until a steady value of the overall separation $S_0$ was reached while operating the column under total reflux. Then, the product withdrawal system was activated to withdraw the gas from the enriched end at a constant and measurable rate. The withdrawal system was built with Pyrex using the design of M.S.K.T. (*8*). Fluctuations of the product withdrawal rate were less than 4% of the magnitude over a period of a few days. During the withdrawal period, decrease of the overall separation was monitored again by processing and analyzing the sample from both ends until a new steady state was reached.

The partial pressure of $NO_2$ in the gas phase was determined a few times during each run by very slowly filling a thermostatted 3.2 cm path length cell (SPC) up to the system's total pressure, and determining the absorbance at 477.0 nm.

The waste $H_2SO_4$ was checked periodically for nitrogen content by using Norwitz's colorimetric method (*18*) which offers a detection limit of 2 ppm for the oxyacids and oxides of nitrogen. All samples tested contained less than 5 ppm of nitrogen.



## Data Reduction

The effective single-stage separation factor, $\alpha_{eff} \equiv 1 + \varepsilon$, and the HETP were determined from the steady-state value of the overall separation under total reflux, $S_0$, and the one while the product was being withdrawn, $S_p$, at a rate of $P$ mmol N/min and by using Cohen's theory for the close separation in square cascade. The overall separations $S$ were calculated as

$$S = (^{15}N/^{14}N)_{bottom}/(^{15}N/^{14}N)_{top} \tag{1}$$

The approach to the asymptotes, $S_0$ and $S_p$, are illustrated in Fig. 2. Solution (19,8) of the equation,

$$S_0^{-|(1+\theta)/[1-(P/L)]|} = \frac{1+\theta}{S_p} - \theta \tag{2}$$

for $\theta$ led to $\varepsilon$:

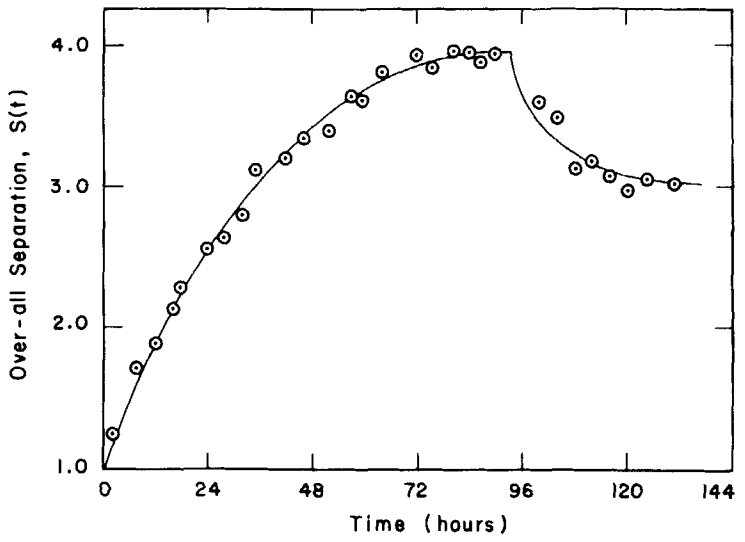


FIG. 2. Overall separation as a function of time for Run 16. Points up to 96 h were taken under total reflux. Points thereafter were observed at $P = 0.207$ mmol N/min.



$$\theta \equiv P/(L\varepsilon) \tag{3}$$

where $L$ is the interstage flow rate in mmol N/min. Solution of $S_0 = \alpha_{\text{eff}}^n$ for the number of separation stages, $n$, yielded the HETP. The volume flow rate of liquid, $\lambda$ (mL/min), obtained by the measuring cup method was transformed to $L$ by using a material balance requirement:

$$L = 1000\lambda d/[G_1 + x(G_2 - G_1)] \tag{4}$$

where $x$ is the atom fraction of nitrogen atoms in the liquid phase that are in the +4 oxidation state, $d$ is the density of the liquid in g/mL, and $G_1$ and $G_2$ are the molecular weights of NO and $NO_2$, respectively. For the purpose of defining $x$, each molecule of $N_2O_3$ was regarded as consisting of one +4 nitrogen atom and one +2 nitrogen atom.

Composition of the liquid, $x$, was calculated from the total pressure $p_t$ and by using Beattie-Vosper vapor pressure equation for liquid $N_2O_3$/$N_2O_4$ systems:

$$\log_{10} p_t\,(\text{torr}) = -\frac{f(x)}{T} + B(x) \tag{5}$$

where $f(x)$ and $B(x)$ are well-tabulated functions (*11, 20*) of $x$. From $x$ the mole fractions of $N_2O_3$ ($x_3$) and $N_2O_4$ ($x_4$) were obtained as $x_3 = 2(1 - x)$ and $x_4 = 2x - 1$.

The liquid mixtures of $N_2O_3$ and $N_2O_4$ behave nearly ideally (*21*). The density, $d$, needed for Eq. (4) was calculated as

$$d(T,x) = x_3 d(T,N_2O_3) + x_4 d(T,N_2O_4) \tag{6}$$

where the values of $d(T,N_2O_3)$ and $d(T,N_2O_4)$ were taken from Shaw and Vosper (*21*) and Addison and Smith (*22*), respectively. Equation (6) also agrees well with Geuther's data (*23*).

The gas-phase compositions were determined from observed values of the total pressure $p_t$ (atm), the temperature $T$, the partial pressure $p_2$ (atm) of $NO_2$, the equilibrium constant for the dissociation of $N_2O_3$ into NO and $NO_2$ ($K_3$), that of $N_2O_4$ into $NO_2$ ($K_4$), and Dalton's law. $K_4$ was calculated by subjecting Bodenstein and Böes' ideal gas equilibrium constant (*24*) to Giauque and Kemp's procedure (*25*) to account for the nonideality. Thus, $K_4$ and $p_2$ yield $p_4$ (atm) of $N_2O_4$. $K_3$, measured by Beattie and Bell (*26*), shows a strong linear dependence on $p_2$. We obtained $K_3$ for our experimental conditions by fitting their data to the functional forms,

$$K_3 = K_3^0 - mp_3, \qquad \log_{10} K_3^0 = -(A_1/T) + B_1$$

$$\log_{10} m = -(A_2/T) + B_2$$

$K_3$, $p_t$, $p_2$, and $p_4$ led to $p_3$ (atm) of $N_2O_3$, and Dalton's law then gave $p_1$ (atm) of NO. Since Dalton's law is one of the most realistic ideal gas laws and because NO was the major gas component under our experimental conditions, $p_1$ obtained by this procedure is little affected by any uncertainties in the assumptions and procedures used to obtain other partial pressures.

## RESULTS AND DISCUSSION

Results of the column experiments are summarized in Table 1. From the extent of effects of product withdrawal rate, $P$, on the overall

TABLE 1
Summary of Exchange Column Experiments[a,b]

| Run | $T$ (°C) | $p_t$ (atm) | $\lambda$ (mL/min) | $L$ (mmol N/min) | $P$ (mmol N/min) | $S_0$ | $S_p$ | $\alpha_{eff}$ | $n$ | HETP (cm) |
|---|---|---|---|---|---|---|---|---|---|---|
| 12A | 20.0 | 1.52 | $0.84_0$ | 27.5 | 0.199 | 2.19 | 1.71 | 1.009 | 87.5 | 0.57 |
| 12B | 20.0 | 2.00 | $0.77_3$ | 26.0 | 0.223 | 2.64 | 2.12 | 1.020 | 49.0 | 1.02 |
| 10A | 15.5 | 1.00 | $0.78_5$ | 25.4 | 0.318 | 1.49 | 1.29 | 1.006 | 66.7 | 0.75 |
| 10B | 15.5 | 1.52 | $0.81_9$ | 27.4 | 0.251 | 2.06 | 1.69 | 1.012 | 60.6 | 0.83 |
| 10C | 15.5 | 2.00 | $0.89_4$ | 30.6 | 0.251 | 2.45 | 2.06 | 1.021 | 43.1 | 1.16 |
| 14 | 15.0 | 2.70 | $0.55_2$ | 19.4 | 0.161 | 3.90 | 2.83 | 1.030 | 46.0 | 1.09 |
| 15 | 14.5 | 3.40 | $0.69_5$ | 24.8 | 0.179 | 4.15 | 3.07 | 1.032 | 45.2 | 1.11 |
| 16 | 15.0 | 4.10 | $0.91_3$ | 32.9 | 0.207 | 3.98 | 3.05 | 1.030 | 46.7 | 1.07 |
| 7B | 14.0 | 1.00 | $0.56_5$ | 18.4 | 0.104 | 1.82 | 1.64 | 1.010 | 60.2 | 0.83 |
| 5[c] | 5.0 | 1.00 | $0.73_0$ | 24.8 | 0.152 | 7.04 | 3.40 | 1.020 | 98.6 | 1.01 |
| 9 | −4.0 | 1.00 | $0.97_6$ | 34.4 | 0.167 | 4.40 | 3.40 | 1.029 | 51.8 | 0.97 |
| 11 | −4.0 | 1.58 | $0.86_3$ | 31.1 | 0.173 | 3.90 | 3.05 | 1.028 | 49.3 | 1.01 |
| 7A | −9.0 | 1.00 | $0.66_4$ | 23.9 | 0.102 | 5.70 | 4.30 | 1.036 | 49.2 | 1.02 |

[a]All runs except Run 5 were carried out using an exchange column (50 cm long × 1.55 cm i.d.) packed with Podbielniak SS Helipak No. 3013.

[b]Table headings are: $T$ = exchange column temperature; $p_t$ = total pressure; $\lambda$ = liquid flow rate; $L$ = interstage flow rate in exchange column; $P$ = product withdrawal rate during the product withdrawal experiments; $S_0$ = steady-state value of the overall separation under total reflux; $S_p$ = steady-state value of the overall separation at the product withdrawal rate of $P$; $\alpha_{eff} = 1 + \varepsilon_{eff}$; $n$ = number of separative stages in the exchange column used; HETP = height equivalent of theoretical plates = (packed column length)/$n$.

[c]For Run 5, a column 100 cm long and 0.95 cm in i.d. with the same packing was used.

separation shown in the table, it is seen that a loss of enriched nitrogen via the sulfuric acid effluent from the refluxer at a rate of (5 μg N/mL) × (3 mL $H_2SO_4$/min) or 0.001 mmol N/min would affect the overall separation only by 0.1% of its magnitude.

## Single-Stage Separation Factor

Present values of $\alpha_{eff}$ under atmospheric pressure compare fairly well with the values obtained by M.S.K.T. (*8*). Both results show an increasing trend of $\alpha_{eff}$ with temperature, and the present results fall generally between M.S.K.T.'s results of column experiments and those of the single-stage equilibration measurements.

Table 2 presents a summary of chemical compositions ($x$) of the liquid phase and those of the gas phase obtained by the procedures described earlier. The overall atom fraction, $y$, of +4 nitrogen in the gas phase was computed as

$$y = (p_2 + p_3 + 2p_4)/(p_1 + p_2 + 2p_3 + 2p_4) \quad (7)$$

The separation factor due to a single isotope exchange reaction usually increases with decreasing temperature, although a number of exceptions have been noted in the past (*27*). At the present experimental temperatures, the reduced partition function ratios (*28*), (RPFR) or $(s/s')f$, of all $^{15}N$-for-$^{14}N$ substitutions in all oxides of nitrogen do increase with decreasing temperature. Both temperature and pressure affect the chemical compositions, and the gas-phase composition varies significantly more rapidly than the liquid composition. In particular, an increase in pressure results in a rapid increase in the gas-phase mole fraction of NO, the species which has the smallest RPFR of all oxides of nitrogen.

In Fig. 3, $\alpha_{eff}$ of all runs, i.e., those obtained at all temperatures and pressures, have been plotted as a function of $y$. The reasonably good correlation between these quantities suggests that, within the range of temperatures studied, the observed changes in $\alpha_{eff}$ are due more to changes in the chemical composition than to variations in the quantum mechanical distribution of isotopes among the exchanging chemical species.

Figure 4 illustrates the typical behavior of $\alpha_{eff}$ as a function of pressure: At a given temperature, $\alpha_{eff}$ levels off after an initial rise with increasing pressure. The asymptote is approached as the chemical compositions of both phases become insensitive to the total pressure (cf. Fig. 5).

TABLE 2
Liquid and Gas Chemical Compositions[a]

| Run | $T$ (°C) | $p_t$ (atm) | $p_1$ (atm) | $p_2$ (atm) | $p_3$ (atm) | $p_4$ (atm) | $x$ | $y$ | $p_t'$ (atm) | $LV_g$ (mL/min) |
|---|---|---|---|---|---|---|---|---|---|---|
| 12B | 20.0 | 2.10 | $1.43_2$ | $0.15_3$ | $0.24_4$ | $0.26_6$ | 0.77 | 0.36 | 2.61 | 240 |
| 10A | 15.5 | 1.02 | $0.28_0$ | $0.16_5$ | $0.08_6$ | $0.49_2$ | 0.91 | 0.77 | 1.60 | 376 |
| 10B | 15.5 | 1.50 | $0.77_4$ | $0.14_9$ | $0.19_2$ | $0.38_6$ | 0.80 | 0.53 | 2.08 | 312 |
| 10C | 15.5 | 2.00 | $1.36_0$ | $0.12_5$ | $0.25_5$ | $0.27_1$ | 0.73 | 0.36 | 2.54 | 286 |
| 14 | 15.0 | 2.68 | $2.18_8$ | $0.09_2$ | $0.26_1$ | $0.14_3$ | 0.66 | 0.21 | 3.09 | 149 |
| 15 | 14.5 | 3.40 | $2.92_4$ | $0.07_8$ | $0.29_2$ | $0.10_7$ | 0.61 | 0.15 | 3.80 | 154 |
| 16 | 15.0 | 4.08 | $3.59_7$ | $0.07_3$ | $0.32_1$ | $0.09_1$ | 0.58 | 0.13 | 4.49 | 173 |
| 9 | −4.0 | 1.00 | $0.84_0$ | $0.02_5$ | $0.08_0$ | $0.05_9$ | 0.67 | 0.19 | 1.14 | 665 |
| 11 | −4.0 | 1.60 | $1.36_0$ | $0.02_8$ | $0.14_4$ | $0.07_1$ | 0.59 | 0.17 | 1.82 | 378 |

[a] $p_1$, $p_2$, $p_3$, and $p_4$ are the partial pressures of NO, $NO_2$, $N_2O_3$, and $N_2O_4$, respectively. $x$ and $y$ are the atom fractions of the +4 nitrogen atoms in the liquid and gas phases, respectively. $V_g$ is the volume of gas containing 1 mmol of nitrogen atoms as computed by using Eq. (9), and $p_t'$ is the effective gas pressure defined in Eq. (9).

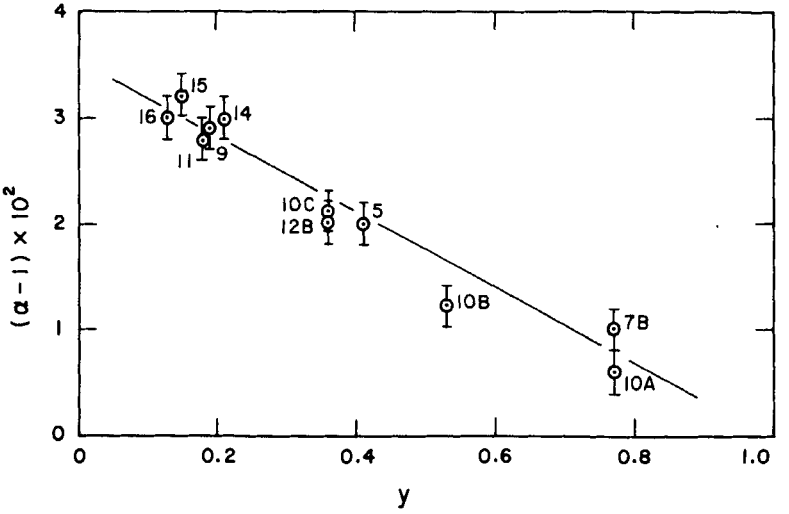


FIG. 3. Correlation between $\alpha_{eff}$ and $y$.



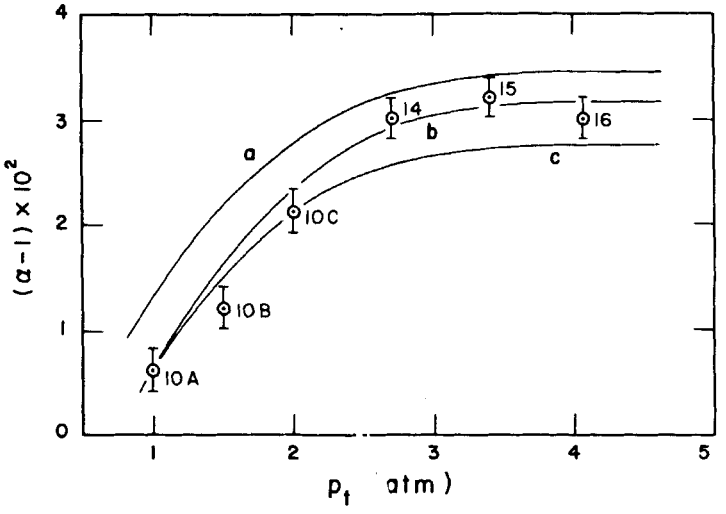


FIG. 4. $\alpha_{eff}$ as a function of total pressure at 1 . Curve a, calculated by Monse and co-workers (*17*); Curve b, calculated from new F- rix Set 1 (see text); Curve c, calculated from new F-matrix . (see text).

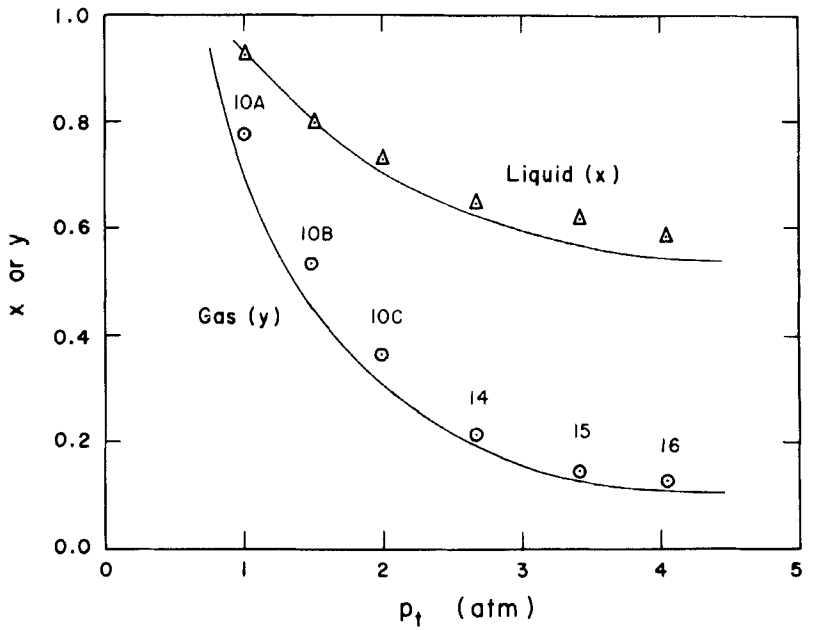


FIG. 5. Equilibrium compositions of liquid ($x$) and vapor ($y$) as functions of total pressure at 15°C. Circles: Gas phase composition, present work (see text). Triangles: Liquid phase composition, computed from Eq. (5). Solid curves: Extrapolated from Purcell and Cheesman, *J. Chem. Soc.*, p. 826 (1932).



Three curves in Fig. 4 were calculated by using three alternative sets of F-matrices and the equation

$$\alpha_{\text{eff}} = [\sum_i x_i(s/s')f_i]_{\text{liquid}}/[\sum_j y_j(s/s')f_j]_{\text{gas}} \tag{8}$$

where the mole fractions of the gas phase species, $y_j$ ($j = 1 \sim 4$), were obtained as $y_j = p_j/p_t$. Since the original calculations of $\alpha_{\text{eff}}$ (Curve a in Fig. 4) were made by Monse (*17*), new data on various isotopic molecules of $N_2O_3$ and $N_2O_4$ have been published representing results of new techniques such as laser IR and Raman spectroscopies and matrix isolation methods. We have reduced these data to two new sets of F-matrices.

For NO and $NO_2$ the F-matrices of Monse, Spindel, and Stern (*29*) were used. The F-matrices of gas and liquid $N_2O_4$ were fit to Begun and Fletcher's (*30*) observed fundamentals with an exception for $\nu_{10}$ ($NO_2$

rock), for which the gaseous $^{14}N_2O_4$ data by Bibart and Ewing (*31*) (270 $cm^{-1}$) and the solid $^{14}N_2O_4$ data by Andrews and Anderson (*32*) (265 $cm^{-1}$) were employed. The **F**-matrix for the in-plane vibrations of gaseous asymmetric $N_2O_3$ was formulated to reproduce the $\nu_1 \sim \nu_5$ fundamentals of all isotopic $N_2O_3$ molecules obtained by means of the $N_2$ matrix isolation method by Varetti and Pimentel (*33*), and $\nu_6 = 260$ $cm^{-1}$ and $\nu_7 = 160$ $cm^{-1}$ from Bradley et al. (*34*). The matrix for the in-plane vibrations of liquid $N_2O_3$ was obtained by fitting Hisatsune's data (*35*) on solid $^{14}N_2O_3$ and $^{15}N_2O_3$.

The two new sets of **F**-matrices mentioned earlier differ from each other only in the **F**-matrices for the out-of-plane vibrations of $N_2O_3$. Set 1 was fit to $\nu_8$ ($NO_2$ out-of-plane wag) values of 627 $cm^{-1}$ ($^{14}N_2O_3$) and 614 $cm^{-1}$ ($^{15}N_2O_3$) obtained by Hisatsune (*35*) and $\nu_9$ (torsion) = 76 $cm^{-1}$ from Bradley et al. (*34*). Set 2 was obtained to reproduce $\nu_8 = 337$ $cm^{-1}$ ($^{14}N_2O_3$) and $\nu_9 = 63$ $cm^{-1}$ ($^{14}N_2O_3$) observed by Bibart and Ewing (*36*). All frequencies of $N_2O_3$ and $N_2O_4$ molecules calculated from these **F**-matrices are within 2 $cm^{-1}$ of all observed fundamentals. Since there seemed to be a controversy on the assignment of $\nu_8$ of $N_2O_3$ at the time of our calculation, we tried both sets. In Fig. 4, Curves b and c were drawn from calculations using the **F**-matrix Sets 1 and 2, respectively. Set 1 is seen to agree with the present experimental data on $\alpha_{eff}$ much better than Set 2. This observation is in agreement with a recent laser Raman measurement by Nour, Chen, and Laane (*37*). It is interesting to note that measurements of thermodynamic quantities such as $\alpha_{eff}$ seem to provide auxiliary information useful in the frequency assignment.



## HETP

The behavior of HETP is less straightforward. For instance, the HETP's of Runs 10A, 10B, 10C, 14, 15 and 16, all at 15°C, show no systematic trend relative to variations in the interstage flow rate $L$ (Table 1). As a function of pressure ($p_t$) at 15°C, HETP increases sharply up to about 2 atm, at which point it abruptly levels off. It is inconceivable that this is due to reduced exchange reaction rates caused by the lowering of +4 nitrogen concentration in the gas phase. Although the isotope exchange reactions among various nitrogen oxides in the gas phase had been shown to proceed more rapidly with increasing concentrations of +4 nitrogen (*38*), the concentrations of +4 nitrogen needed for the significantly fast catalysis is several orders of magnitude lower than the lowest +4 nitrogen concentration ($y$) used in the present study.

The observed behavior of HETP can be rationalized on the basis of the

linear flow rates of gas stream. Under total or near total reflux, HETP should depend on the linear flow rate of the gas phase. Given a liquid flow rate, the gas rate is affected by any process parameters that influence the gas-phase chemical composition.

Let $V_g$ be the gas phase volume (mL) that contains 1 mmol of nitrogen atoms at the $p_t$ and $T$ of the exchange column. Then, on the basis of ideal gas law,

$$V_g = \frac{RT}{(p_1 + p_2 + 2p_3 + 2p_4)} \equiv \frac{RT}{p_t} \tag{9}$$

In Fig. 6 the HETP's of the runs carried out at 15.0 ± 0.5°C and those at −4°C have been plotted against $LV_g$, a quantity which the linear gas flow rate is proportional to. The HETP linearly decreases with increasing $LV_g$ at 15°C (*39*), except for Run 10C which must be a result of poor wetting of the column packing. The large negative slope implies that the overall



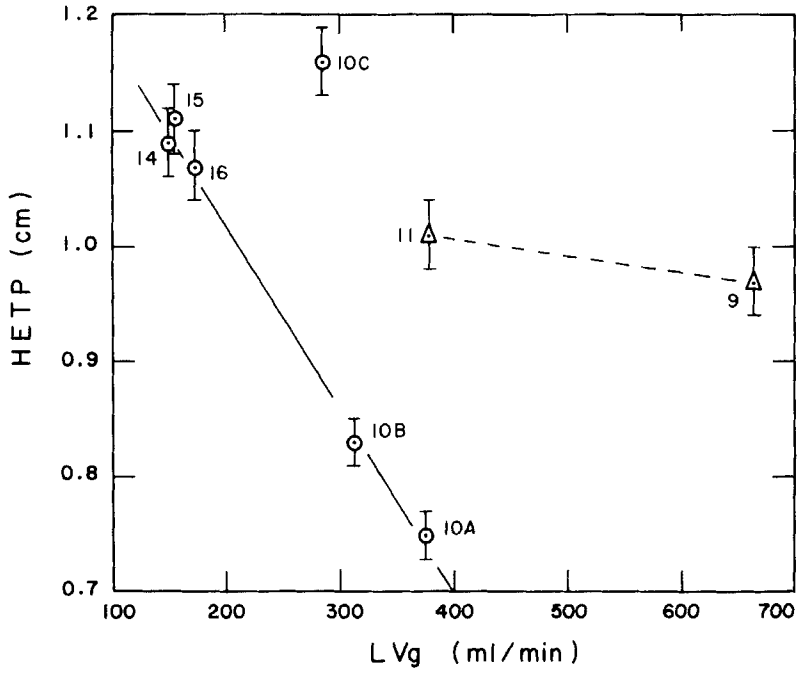


FIG. 6. Correlation between HETP and gas flow rate. Solid line: At 15°C. Dashed line: At −4°C.

exchange rates in these runs are dominantly diffusion-controlled. This correlation should be valid as long as the temperature is 15.0 ± 0.5°C and the flow rates remain within the range shown in Fig. 6. Thus, if the flow rates of Runs 14, 15, and 16 are increased two- to threefold, they should yield much smaller HETP's and shorter process times. At −4°C the effect of the lower reaction rate becomes more significant than at the higher temperature, resulting in a less significant influence of the flow rate.

## Approach to Steady State

An important characteristic of the isotope fractionation system is the rate of approach to the steady state, since it determines the length of nonproductive time period, which is usually long mainly due to the generally small separation factor. The rate under total reflux is a function of $\alpha_{eff}$, $n$, $L$, the holdup in the exchange column ($H_c$), and that in the product end ($H_r$). The latter includes the refluxer system. The data, such as the ones plotted in Fig. 2, have been fitted to Cohen's theory (*19*) using a refined table of parameters prepared by Wieck and Ishida (*40*). It can be shown that these procedures on the present data determine the holdup ratio, $H_r/H_c$, to a precision of ±0.02 and the holdup by the exchanger, $H_c$, to a relative precision of 1%. The results are summarized in Table 3. The relatively small holdup ratios obtained at the higher pressure is attributable to the narrower reflux reaction zone due to the higher temperature.



TABLE 3
Summary of Holdup Calculations[a]

| Run | $T$ (°C) | $p_t$ (atm) | Holdups (mmol N) $H_r$ | Holdups (mmol N) $H_c$ | Holdup ratio $K/\lambda_0 n$ |
|---|---|---|---|---|---|
| 9 | −4.0 | 1.00 | 87 | 870 | 0.10 |
| 11 | −4.0 | 1.58 | 180 | 710 | 0.25 |
| 12A | 20.0 | 1.52 | 26 | 510 | 0.05 |
| 14 | 15.0 | 2.70 | 49 | 930 | 0.05 |
| 15 | 14.5 | 3.40 | 77 | 1600 | 0.05 |

[a] $H_r$ = holdup in the product end which includes the product refluxer; $H_c$ = total holdup by the exchange column = $\lambda_0 nL$; $\lambda_0$ = holdup per stage divided by $L$; $K/\lambda_0 n$ = holdup ratio = $H_r/H_c$; $K \equiv H_r/L$.

TABLE 4
Comparison of Effects of Operating Parameters on the Size of $NO/NO_3$ Single Exchange Column System: Basis = 1 g of 99% $^{15}N$/day[a]

| | 7A | 10A | 15 | 16 | 12B |
|---|---|---|---|---|---|
| Operating conditions: | | | | | |
| $T$ (°C) | −9 | +15.5 | +14.5 | +15.0 | +20.0 |
| $p_t$ (atm) | 1.00 | 1.00 | 3.40 | 4.08 | 2.00 |
| $\lambda/A$ (mL/cm$^2$ · min) | 0.35 | 0.42 | 0.37 | 0.48 | 0.42 |
| $L/A$ (mmol N/cm$^2$ · min) | 12.7 | 13.5 | 13.1 | 17.4 | 13.8 |
| Parameters obtained: | | | | | |
| $\alpha_{eff}$ | 1.36 | 1.006 | 1.032 | 1.030 | 1.020 |
| HETP | 1.02 | 0.75 | 1.11 | 1.07 | 1.02 |
| Minimum required parameters: | | | | | |
| $n_{min}$ | 289 | 1706 | 324 | 345 | 515 |
| $(L/P)_{min} \times 10^{-3}$ | 7.81 | 45.5 | 8.75 | 9.31 | 13.8 |
| $L_{min}$ (mmol N/min) | 361 | 2105 | 405 | 431 | 640 |
| $H_{min}$ (cm) | 295 | 1280 | 360 | 369 | 525 |
| $A_{min}$ (cm$^2$) | 28.4 | 157 | 30.9 | 24.8 | 46.0 |
| $V_{min}$ (cm$^3$) | $8.4 \times 10^3$ | $2.0 \times 10^5$ | $1.1 \times 10^4$ | $9.2 \times 10^3$ | $2.4 \times 10^4$ |

[a]$\lambda$ = liquid flow rate (mL/min); $A$ = inside cross-sectional area of the exchange column (cm$^2$); $L$ = interstage flow rate (mmol N/min); $n_{min}$ = minimum number of stages; $(L/P)_{min}$ = minimum reflux ratio; $L_{min}$ = minimum interstage flow (mmol N/min); $H_{min}$ = minimum height of exchange column = $(n_{min})$ (HETP); $A_{min}$ = minimum inside cross-sectional area of exchange column = $L_{min}/(L/A)$; $V_{min}$ = minimum inside volume = $(H_{min})(A_{min})$.

## Effects of Process Parameters on the Column Size

The sizes of single exchange column systems needed for production of 1 g/day of 99% $^{15}N$ were calculated by scaling up the present column and using the experimental conditions of several runs reported in this paper. The results are compared in Table 4. The minimum number of stages, $n_{min}$, and the minimum reflux ratio, $(L/P)_{min}$, were computed by using the formula (*1*),

$$n_{min} = (\ln S_0)/(\alpha_{eff} - 1) \tag{10}$$

and

$$(L/P)_{min} \simeq (N_p - N_f)/[(\alpha_{eff} - 1)N_f(1 - N_f)] \tag{11}$$

where $N_p$ is the atom fraction of $^{15}N$ in the product, i.e., 0.99, $N_f$ is the atom fraction of $^{15}N$ in the feed, i.e., 0.00365, and $S_0$ corresponds to $^{15}N_{bottom} = 0.99$ and $^{15}N_{top} = 0.00365$.

Table 4 shows that a twentyfold reduction in the column volume is obtained by increasing the pressure from 1 to 4 atm at 15°C and that the column volume at −9°C and atmospheric pressure is approximately the same as that obtained at +15°C and 4 atm. The Fig. 6 correlation predicts that, at 15°C and under a few atmospheres, a two- to threefold increase in the flow rate will produce a 30 to 70% reduction in the HETP. The combined effects of such an increased flow rate on $H_{min}$ and $A_{min}$ would result in an overall volume reduction by a factor of 50 to 100 relative to the atmospheric operations at the same temperature.

In Table 5 the column sizes of the $NO/N_2O_3$ systems, calculated on the basis of the data of Run 15 (but with the higher flow rates by factors of 2 and 3) and the correlation of Fig. 6, are compared to those for the $NO/HNO_3$ system (*8*). Both data are the result of the direct scale-up and do not include any factors to account for reduced efficiencies and other engineering nonidealities. It is clearly seen that, although $\alpha_{eff}$ of the $NO/N_2O_3$ system is smaller than that of the Nitrox system, the HETP of the former system is so favorable that the overall column volume of this system could be considerably smaller than that of the Nitrox system.

The similar trend of decreasing HETP with increasing $LV_g$ is apparent at 20°C when one compares Runs 12A and 12B in Table 1: As $p_t$ increases, $p_t'$ also increases (Table 2 and Eq. 9), and $V_g$ decreases consequently. It is thus interesting to explore the behaviors of HETP of

TABLE 5
Comparison of the $NO/N_2O_3$ System and the Nitrox System[a]

| | $NO/HNO_3$[b] | | | $NO/N_2O_3$[c] | | |
|---|---|---|---|---|---|---|
| Operating parameters: | | | | | | |
| $T$ (°C) | | 25 | | | 14.5 | |
| $P_t$ (atm) | | 1 | | | 3.5 | |
| $\lambda/A$ (mL/cm$^2$ · min) | 1.6 | 3.0 | 5.0 | 0 | 0.75[d] | 1.1[d] |
| $L/A$ (mmol N/cm$^2$ · min) | 17 | 32 | 53 | 26 | | 39 |
| $\alpha_{eff}$ | | 1.055 | | | 1.032 | |
| HETP | 2.8 | 4.0 | 5.8 | 0.85 | | 0.60 |
| Minimum required parameters: | | | | | | |
| $n_{min}$ | | 191 | | | 324 | |
| $(L/P)_{min} \times 10^{-3}$ | | 4.90 | | | 8.75 | |
| $L_{min}$ (mmol N/min) | | 228 | | | 405 | |
| $H_{min}$ (cm) | 535 | 764 | 1100 | 275 | | 194 |
| $A_{min}$ (cm$^2$) | 13 | 7.1 | 4.3 | 15.6 | | 10.4 |
| $V_{min} \times 10^{-3}$ (cm$^3$) | 7.2 | 5.4 | 4.8 | 4.3 | | 2.0 |

[a]For the symbols used, see the footnote in Table 4.
[b]From Ref. 8.
[c]Based on Run 15, present work.
[d]$\lambda/A$ = 0.75 mL/cm$^2$ · min corresponds to twice the value of $\lambda/A$ used in Run 15. $\lambda/A$ = 1.1 mL/cm$^2$ · min corresponds to three times the value of $\lambda/A$ used in Run 15. The HETP values for each flow rate were obtained by interpolation and extrapolation of the correlation of Fig. 6.



the $NO/N_2O_3$ system at even higher temperatures and elevated pressures.

## CONCLUSION

It has been shown that, at a given temperature, $\alpha_{eff}$ increases with pressure primarily due to the increase in the partial pressure of nitric oxide, and $\alpha_{eff}$ levels off as the chemical compositions approach their high pressure asymptotic limits. At 15°C this occurs at 3~4 atm. The presently obtained $\alpha_{eff}$ agrees well with recent spectroscopic data. The observed HETP's correlate well with the linear gas flow rates. It is predicted that the $NO/N_2O_3$ system operated at 15°C and under 3~4 atm would offer considerably smaller plant volumes than the Nitrox system, primarily on the strength of its HETP. The HETP can be smaller than that of the Nitrox system by factors of 7 to 10. It seems worthwhile to study this system at temperatures closer to the ambient temperature.

## Acknowledgments

We are grateful for the assistance rendered by Arundhati Kanungo and Mohammed Bahavar in taking shifts during long periods of column operations.

Research supported by the Office of Basic Energy Sciences, U.S. Department of Energy, Contract No. DE-AC02-80ER10612.



## REFERENCES

1. M. Benedict, T. H. Pigford, and H. W. Levi, *Nuclear Chemical Engineering*, 2nd ed., McGraw-Hill, New York, 1981.
2. W. P. Barthold, Trans. Am. Nucl. Soc., *21*, 407 (1975).
3. V. J. Tennery, E. S. Bomar, W. D. Bond, S. V. Kaye, L. E. Morse, and J. E. Till, *U.S. ERDA Report ORNL/TM-5538*, June 1976.
4. V. J. Tennery, *U.S. ERDA Report ORNL/TM-5621*, November 1976.
5. H. C. Urey and L. J. Grieff, *J. Am. Chem. Soc.*, *5*, 321 (1935).
6. T. I. Taylor and W. Spindel, *J. Chem. Phys.*, *16*, 635 (1948).
7. W. Spindel and T. I. Taylor, *Ibid.*, *23*, 981 (1955).
8. E. U. Monse, W. Spindel, L. N. Kauder, and T. I. Taylor, *Ibid.*, *32*, 1557 (1960).
9. E. U. Monse, T. I. Taylor, and W. Spindel, *J. Phys. Chem.*, *65*, 625 (1961).
10. E. U. Monse, L. N. Kauder, and W. Spindel, *Z. Naturforsch.*, *18a*, 235 (1963).
11. I. R. Beattie and A. J. Vosper, *J. Chem. Soc.*, p. 4799 (1960).
12. A. J. Vosper, *J. Chem. Soc., A*, p. 1589 (1971).
13. W. Spindel and T. I. Taylor, *J. Chem. Phys.*, *24*, 626 (1956).
14. W. Spindel and T. I. Taylor, *Trans. N. Y. Acad. Sci. 19*, 3 (1956).
15. T. I. Taylor and W. Spindel, in *Proceedings of International Symposium on Isotope Separation*, North-Holland, Amsterdam, 1958, p. 158.
16. T. Ishida and W. Spindel, *J. Chem. Eng. Data, 15*, 107 (1970).
17. E. U. Monse, *J. Chem. Phys.*, *33*, 312 (1960); E. U. Monse, L. N. Kauder, and W. Spindel, *Ibid.*, *41*, 3898 (1964).
18. G. Norwitz, *Anal. Chem.*, *34*, 227 (1962).
19. K. Cohen, *J. Chem. Phys.*, *8*, 588 (1940); *Theory of Isotope Separation*, McGraw-Hill, New York, 1951.
20. A. J. Vosper, *J. Chem. Soc., A*, p. 1762 (1966).
21. A. W. Shaw and A. J. Vosper, *Ibid.*, p. 2708 (1971).
22. C. C. Addison and B. C. Smith, *J. Chem. Soc.*, p. 3664 (1958).
23. A. Geuther, *Ann. Chem.*, *246*, 96 (1888).
24. M. Bodenstein and F. Böes, *Z. Phys. Chem.*, *100*, 75 (1922).
25. W. F. Giauque and J. D. Kemp, *J. Chem. Phys.*, *6*, 40 (1938).
26. I. R. Beattie and S. W. Bell, *J. Chem., Soc.*, p. 1681 (1957).
27. M. J. Stern, W. Spindel, and E. U. Monse, *J. Chem. Phys.*, *48*, 2908 (1968); W. Spindel, M. J. Stern, and E. U. Monse, *Ibid.*, *52*, 2022 (1970).
28. J. Bigeleisen and M. G. Mayer, *Ibid.*, *15*, 216 (1947).
29. E. U. Monse, W. Spindel, and M. J. Stern, *Adv. Chem., Ser.*, *89*, 185 (1969).
30. G. M. Begun and W. H. Fletcher, *J. Mol. Spectrosc.*, *4*, 388 (1960).
31. C. H. Bibart and G. E. Ewing, *J. Chem. Phys.*, *61*, 1284 (1974).

32. B. Andrews and A. Anderson, *Ibid., 74*, 3 (1981).
33. E. L. Varetti and G. C. Pimentel, *Ibid., 55*, 3813 (1971).
34. G. M. Bradley, W. Sidall, H. Strauss, and E. L. Varetti, *J. Phys. Chem., 79*, 1949 (1975).
35. I. C. Hisatsune, J. P. Devlin, and Y. Wasa, *J. Chem. Phys., 33*, 714 (1960).
36. C. H. Bibart and G. E. Ewing, *Ibid., 55*, 3813 (1971).
37. E. M. Nour, L. H. Chen, and J. Laane, *J. Phys. Chem., 87*, 1113 (1983).
38. W. Spindel and M. J. Stern, *J. Chem. Phys., 32*, 1579 (1960); F. S. Klein, W. Spindel, and M. J. Stern, *J. Chim. Phys., 60*, 148 (1963), and the references therein.
39. To be exact, the HETP should be correlated to $(L - P)V_g$, but $LV_g$ is a satisfactory approximation for this for the present experimental conditions.
40. H. Wieck and T. Ishida, *Sep. Sci., 12*, 587 (1977).

*Received by editor March 4, 1985*